Extension and comparison of neoclassical models for poloidal rotation in tokamaks

W. M. Stacey
Fusion Research Center, Georgia Institute of Technology, Atlanta, Georgia 30332, USA

(Received 19 September 2007; accepted 6 December 2007; published online 18 January 2008)

Several neoclassical models for the calculation of poloidal rotation in tokamaks were rederived within a common framework, extended to include additional physics and numerically compared. The importance of new physics phenomena not usually included in poloidal rotation calculations (e.g., poloidal electric field, $\mathbf{V}\times\mathbf{B}$ force resulting from enhanced radial particle flow arising from the ionization of recycling neutrals) was examined. Extensions of the Hirshman–Sigmar, Kim–Diamond–Groebner, and Stacey–Sigmar poloidal rotation models are presented. © *2008 American Institute of Physics*. [DOI: 10.1063/1.2829073]

I. INTRODUCTION

Poloidal rotation is of intrinsic interest for what it reveals about parallel viscous momentum transport and also because it appears to play a role in the shear suppression of turbulent energy transport. There are a number of theoretical models for the calculation of poloidal rotation that are referred to as "neoclassical," ranging from the early prediction by Hazeltine[1] of an ion poloidal rotation velocity proportional to the ion radial temperature gradient through the several variants of the Hirshman–Sigmar fluid model[2] (in which the ion poloidal rotation is calculated from a balance between parallel frictional and viscous forces) to the Stacey–Sigmar model[3] (in which the poloidal rotation is calculated from the poloidal momentum balance using a rate-of-strain tensor formulation for the viscous force).

The purposes of this paper are to place these various models within a common framework, to extend them to represent additional phenomena, and to present numerical calculations comparing the predictions of the various models and illustrating the importance of various phenomena to the calculation of poloidal rotation. To this end, the various models are derived within the common framework of fluid momentum balance, with kinetic theory effects incorporated via constitutive relations (i.e., the Hirshman–Sigmar fluid formulation). The various theoretical models then follow from various choices of the viscous force formulation and from the retention of various terms in the poloidal momentum balance. Extensions of the theories for poloidal rotation previously developed by Hirshman–Sigmar,[2] Kim–Diamond–Groebner,[4] and Stacey–Sigmar[3] are suggested by such an approach.

The paper is organized as follows. The fluid poloidal momentum balance is formulated in Sec. II. The Hirshman–Sigmar formulation of the parallel viscous force is summarized in Sec. III, where it is shown that the Hazeltine,[1] Kim–Diamond–Groebner,[4] and NCLASS[5] versions of poloidal rotation theory are obtained by using the Hirshman–Sigmar viscous force and retaining different terms in the poloidal momentum balance equation. The Stacey–Sigmar representation of the parallel viscous force in terms of a rate-of-strain tensor is described and extended to include heat flux as well as flow terms in Sec. IV. In Sec. V, the Hirshman–Sigmar poloidal rotation theory is extended by retaining additional terms in the poloidal momentum balance equation. Numerical predictions of the various poloidal rotation theories are compared and the effect of retaining various terms in the momentum balance equation is examined in Sec. VI. Finally, the work is summarized in Sec. VII.

II. POLOIDAL MOMENTUM BALANCE

Poloidal rotation in tokamak plasmas is governed by the poloidal component of the momentum balance equation,

$$n_j m_j[(\boldsymbol{v}_j\cdot\nabla)\boldsymbol{v}_j]_\theta + [\nabla\cdot\Pi_j]_\theta + \frac{1}{r}\frac{\partial p_j}{\partial\theta} - M_{\theta j} + n_j m_j \nu_{jk}(v_{\theta j} - v_{\theta k}) + n_j e_j (v_{rj}B_\phi - E_\theta) + n_j m_j \nu_{ionj} v_{\theta j} + n_j m_j \nu_{elcxj} v_{\theta j} = 0, \tag{1}$$

where the poloidal component of the inertial term has been written as

$$[\nabla\cdot(n_j m_j \boldsymbol{v}_j\boldsymbol{v}_j)]_\theta = n_j m_j[(\boldsymbol{v}_j\cdot\nabla)\boldsymbol{v}_j]_\theta + [(\nabla\cdot n_j m_j \boldsymbol{v}_j)\boldsymbol{v}_j]_\theta = n_j m_j[(\boldsymbol{v}_j\cdot\nabla)\boldsymbol{v}_j]_\theta + n_j m_j \nu_{ionj} v_{\theta j} \tag{2}$$

by making use of the continuity equation

$$\nabla\cdot n_j\boldsymbol{v}_j = S_j = n_j\nu_{ionj}. \tag{3}$$

In toroidal geometry, the derivative term in Eq. (2) can be written

$$n_j m_j[(\boldsymbol{v}_j\cdot\nabla)\boldsymbol{v}_j]_\theta = n_j m_j\left[v_{rj}\frac{\partial v_{\theta j}}{\partial r} + \frac{v_{rj}v_{\theta j}}{r} + \frac{1}{2}\frac{1}{r}\frac{\partial v_{\theta j}^2}{\partial\theta} + \frac{v_{\phi j}^2}{R}\sin\theta\right]. \tag{4}$$

The second term in Eq. (1) is the viscous force, the third term is the pressure gradient, the fourth term represents any external poloidal momentum input, the fifth term is the collisional friction term, the sixth term is a combination of the $\mathbf{V}\times\mathbf{B}$ force and the electric field force, the seventh term was introduced in simplifying the inertial term, and the last term

represents the poloidal momentum damping due to charge exchange and elastic scattering of rotating ions with nonrotating neutrals.

Various neoclassical models of poloidal rotation differ by which terms are retained in the momentum balance of Eq. (1) and in the representation of the viscous force (and friction) term.

A theoretical framework will be developed for a two-species "ion-impurity" plasma, for simplicity; it is readily extendable to multiple ion species by summing the friction term over all other ion species and by summing over all ion species in calculating the electron density from charge neutrality. In a similar vein, a simple Lorentz form of the friction term will be used in order not to further complicate the formalism and because poloidal temperature gradient contributions would not be expected to be significant.

III. HIRSHMAN–SIGMAR POLOIDAL ROTATION THEORY

Perhaps the most familiar representation of the poloidal viscous force (or poloidal component of the parallel viscous force) is based on the comprehensive fluid momentum approach developed by Hirshman and Sigmar (HS) (Ref. 2 and other papers in the same time frame) and succinctly summarized by Kim, Diamond, and Groebner (KDG).[4] Following the definitions of Kim *et al.*,[4] the HS FSA (flux surface average) parallel viscous force can be written

$$\langle \mathbf{B}\cdot\nabla\cdot\Pi_{\|}^{j}\rangle^{H\text{-}S} = n_j m_j \nu_{jj}\langle B^2\rangle[\mu_{00}^{j}u_{\theta 0}^{j} + \mu_{01}^{j}u_{\theta 1}^{j}] = n_j m_j \nu_{jj}\langle B^2\rangle \frac{\mu_{00}^{j}}{B_\theta}\left(v_{\theta j} + \frac{B_\phi K^j T_j L_{Tj}^{-1}}{e_j B^2}\right), \quad (5)$$

where $L_x^{-1}\equiv -\partial x/x\partial r$, $K^j \equiv \mu_{01}^j/\mu_{00}^j$, and definitions and formulas for interpolation over collision frequency the μ_{nm}^j are given by Kim *et al.*[4] The first term in the square brackets in Eq. (5) represents the flow contribution and the second term represents the heat flux contribution to the viscous force. The banana (B), plateau (P), and Pfirsch–Schluter (PS) regime values of the transport coefficients for the main ion species are $\mu_{00}^B = 0.53+\alpha$, $\mu_{00}^P = 3.54$, $\mu_{00}^{PS} = (3.02+4.25\alpha)/(2.23+5.32\alpha+2.4\alpha^2)$, where $\alpha \equiv n_z Z^2/n_i$, and the interpolation formula is

$$\mu_{00} = \frac{g\mu_{00}^B}{(1.292\nu_{*j}\mu_{00}^B/\mu_{00}^P)(1+\mu_{00}^P\nu_{*j}\varepsilon^{3/2}/6\mu_{00}^{PS})}, \quad (6)$$

where for the main (deuterium) ion species $\nu_{*i} \equiv \nu_{ii}qR/v_{thi}\varepsilon^{3/2}$ and $g \equiv (1.46\sqrt{\varepsilon}-0.46\varepsilon^{3/2})/(1-1.46\sqrt{\varepsilon}+0.46\varepsilon^{3/2})$ is the ratio of trapped to circulating particles. Because μ_{01} changes signs between regimes, the interpolation formula Eq. (6) is applied for the quantity $K_{01} \equiv \frac{5}{2}\mu_{00} - \mu_{01}$, where for the main ion species $K_{01}^B = 0.71+\alpha$, $K_{01}^P = 10.63$, $K_{01}^{PS} = (12.43+20.13\alpha)/(2.23+5.32\alpha+2.4\alpha^2)$. For the impurity ion species, these same results apply but with $\alpha \to 1/\alpha$, $\nu_{*j} \to \nu_{*k}$.

Different versions of the HS theory of poloidal rotation are obtained by using Eq. (5) for the viscous force but retaining different terms in the poloidal momentum balance Eq. (1). Kim *et al.*[4] retained only the friction and viscous terms in Eq. (1), which yielded the original Hazeltine result[1] derived from kinetic theory for the main ion species "*j*,"

$$v_{\theta j} = B_\phi K^j T_j L_{Tj}^{-1}/e_j B^2, \quad (7)$$

and, in the limit where the impurity viscous force is negligible compared to the impurity-ion friction force (i.e., trace impurities),

$$v_{\theta k} = B_\phi T_j \left[(K^j + 1.5K^k)L_{Tj}^{-1} - L_{pj}^{-1} + \frac{e_j}{e_k}\frac{T_k}{T_j}L_{pk}^{-1}\right] \Big/ e_j B^2 \quad (8)$$

for the impurity ion species "*k*." These two equations will be referred to as the Kim–Diamond–Groebner (KDG) model.

The KDG model can be extended to remove the "trace impurity" limitation by merely retaining the viscous and friction terms for both species in Eq. (1) and using the HS viscous force of Eq. (5) to obtain the coupled set of equations

$$[\nu_{jj}B\mu_{00}^j/B_\theta + \nu_{jk}]v_{\theta j} - [\nu_{jk}]v_{\theta k} = \nu_{jj}\mu_{00}^j \frac{B_\phi}{e_j B B_\theta}K^j T_j L_{Tj}^{-1}$$
$$-[\nu_{kj}]v_{\theta j} + [\nu_{kk}B\mu_{00}^k/B_\theta + \nu_{kj}]v_{\theta k} = \nu_{kk}\mu_{00}^k \frac{B_\phi}{e_k B B_\theta}K^k T_k L_{Tk}^{-1} \quad (9)$$

for the main ion (*j*) and impurity ion (*k*) poloidal velocities. Equations similar to these (but with a more sophisticated treatment of the friction term) are solved in the NCLASS code.[5] A further extension of the HS theory for poloidal rotation will be described in a later section.

IV. STACEY–SIGMAR POLOIDAL ROTATION THEORY

A similar poloidal rotation theory, but one that retained more of the terms in Eq. (1) and used a different viscous force representation that allowed the representation of poloidal asymmetries, was developed in Refs. 3 and 6–8 by Stacey, Sigmar, and co-workers. This theory is summarized and extended in this section.

Shaing and Sigmar[6] made a kinetic theory calculation of the flow contribution to the parallel viscous force (neglecting the heat flux contribution) in a strongly rotating plasma to obtain an expression for the parallel viscous force,

$$\langle \mathbf{B}\cdot\nabla\cdot\Pi_{\|}^{j}\rangle^{Sh\text{-}S} = 3\langle(\hat{n}\cdot\nabla B)^2\rangle\frac{\eta_{0j}}{B_\theta}v_{\theta j}, \quad (10)$$

where $\hat{n} = \mathbf{B}/B$ and $\eta_{0j} = n_j m_j v_{thj} qR f_j(\nu_{jj}^*)$, with $f_j = \varepsilon^{-3/2}\nu_{jj}^*/(1+\varepsilon^{-3/2}\nu_{jj}^*)(1+\nu_{jj}^*)$ being an interpolation formula connecting the collisional result $f_j = 1/\nu_{jj}^*$ to the strongly rotating banana and plateau regime results. Here $\nu_{jj}^* = \nu_{jj}qR/v_{thj}$. The same viscosity formula applies for the main plasma ions and for impurity ions, but evaluated with species-specific parameters. This expression can be extended to include a heat flux contribution to viscosity by analogy with Eq. (5), yielding an extended Shaing–Sigmar form

$$\langle \mathbf{B}\cdot\nabla\cdot\Pi_{\|}^{j}\rangle_{\text{ext}}^{Sh\text{-}S} = 3\langle(\hat{n}\cdot\nabla B)^2\rangle\frac{\eta_{0j}}{B_\theta}\left[v_{\theta j} + \frac{B_\phi K^j T_j L_{Tj}^{-1}}{e_j B^2}\right]. \quad (11)$$

In toroidal coordinates, $\langle(\hat{n}\cdot\nabla B)^2\rangle = 1/2(\varepsilon B/Rq)^2$.

Stacey and Sigmar[7] generalized Braginskii's flow rate-of-strain tensor results[9] to toroidal geometry and replaced the Braginskii collisional viscosity coefficient with the Shaing–

Sigmar viscosity coefficient η_{0j} given above to obtain for the flow contribution to the parallel viscous force

$$\langle \mathbf{B}\cdot\nabla\cdot\Pi_{\|}^{\mathbf{j}}\rangle^{S\text{-}S} = \frac{3}{2}\left\langle \eta_{0j}A_{0j}^{\theta}\frac{\partial B_\theta}{\partial \ell_\theta}\right\rangle \bar{v}_{\theta j} + \frac{3}{2}\left\langle \eta_{0j}A_{0j}^{\phi}\frac{\partial B_\theta}{\partial \ell_\theta}\right\rangle \bar{v}_{\phi j}, \tag{12}$$

where $\ell_\theta \approx r\theta$ is the length element in the poloidal direction, and

$$A_{0j}^{\theta} = 2\left\{ -\frac{1}{3}\left(\frac{\partial v_{\theta j}}{\partial l_\theta}\right) + \left[\left(\frac{1}{R}\right)\frac{\partial R}{\partial l_\theta} + \frac{1}{3}\left(\frac{1}{B_\theta}\right)\frac{\partial B_\theta}{\partial l_\theta}\right] v_{\theta j}\right\} \Big/ \bar{v}_{\theta j} \tag{13a}$$

and, with $f_p \equiv B_\theta/B_\phi$,

$$A_{0j}^{\phi} = 2f_p R\frac{\partial (v_{\phi j}/R)}{\partial l_\theta} \Big/ \bar{v}_{\phi j}. \tag{13b}$$

This form introduced the contribution of poloidal asymmetries in both the poloidal and toroidal velocities (as well as the density) into the parallel viscous force. The overbar on the velocity in Eqs. (12) and (13) distinguishes the FSA quantity from the poloidally varying quantity (the FSA quantity is implied in previous equations). By analogy with Eq. (5), the Stacey–Sigmar (SS) form of the parallel viscous force can be extended to include the neoclassical heat flux contribution,

$$\langle \mathbf{B}\cdot\nabla\cdot\Pi_{\|}^{\mathbf{j}}\rangle_{\text{ext}}^{S\text{-}S} = \frac{3}{2}\left\langle \eta_{0j}A_{0j}^{\theta}\frac{\partial B_\theta}{\partial \ell_\theta}\right\rangle \left[\bar{v}_{\theta j} + \frac{B_\phi K^j T_j L_{Tj}^{-1}}{e_j B^2}\right] + \frac{3}{2}\left\langle \eta_{0j}A_{0j}^{\phi}\frac{\partial B_\theta}{\partial \ell_\theta}\right\rangle \bar{v}_{\phi j}. \tag{14}$$

As mentioned previously, the various versions of neoclassical theory for the calculation of the poloidal rotation velocity are distinguished by which terms are retained in Eq. (1) and which form of the parallel viscous force is used. A more comprehensive formulation of poloidal rotation theory results when all the terms are retained in Eq. (1). We now do this, using the extended SS viscous force of Eq. (14).

In order to treat the poloidal variation over the flux surface, the poloidal density, velocity, and potential asymmetries in the A_{0j} terms are represented with a low-order Fourier expansion,

$$n_j(r,\theta) \approx n_j^0(r)[1 + n_j^c\cos\theta + n_j^s\sin\theta], \tag{15}$$

etc., and Fourier moments of various components of the momentum balance and the continuity equation are used to relate the velocity and electrostatic potential asymmetries to the ion density asymmetries.

The continuity Eq. (3) can be used to relate the poloidal velocity asymmetries to the density asymmetries,

$$\bar{v}_{\theta j}v_{\theta j}^{s} = -n_j^s\bar{v}_{\theta j} + r\bar{\nu}_{\text{ion}j}\frac{\bar{n}_e}{\bar{n}_j}(n_e^c + n_{oj}^c) \tag{16a}$$

and

$$\bar{v}_{\theta j}v_{\theta j}^{c} = -(1+n_j^c)\bar{v}_{\theta j} - r\bar{\nu}_{\text{ion}j}\frac{\bar{n}_e}{\bar{n}_j}(n_e^s + n_{oj}^s), \tag{16b}$$

where $n_e^{s,c}$ and $n_{oj}^{s,c}$ denote asymmetries in the densities of electrons and neutral atoms of species "j," respectively.

The electron poloidal momentum balance (retaining only the pressure and electric field terms) can be used to relate poloidal asymmetries in the electrostatic potential to poloidal asymmetries in the electron density,

$$\Phi^0\Phi^{c,s} = \frac{T_e n_e^{c/s}}{e}. \tag{17}$$

The radial component of the momentum balance for ion species "j,"

$$\frac{\partial p_j}{\partial r} = n_j e_j(E_r + v_{\theta j}B_\phi - v_{\phi j}B_\theta), \tag{18}$$

can be used to relate the poloidal asymmetries in the toroidal velocity to the density asymmetries [using expansions such as Eq. (15) and taking sin and cos moments],

$$\bar{v}_{\phi j}v_{\phi j}^{s} = L_\Phi^{-1}\frac{T_e}{\bar{B}_\theta}n_e^s + r\bar{\nu}_{\text{ion}j}\frac{\bar{n}_e}{\bar{n}_j}f_p^{-1}(n_e^c + n_{oj}^c) - n_j^s\left[2\bar{P}_j' + \bar{v}_{\phi j} - \frac{2\bar{E}_r}{\bar{B}_\theta}\right] \tag{19a}$$

and

$$\bar{v}_{\phi j}v_{\phi j}^{c} = L_\Phi^{-1}\frac{T_e}{\bar{B}_\theta}n_e^c - r\bar{\nu}_{\text{ion}j}\frac{\bar{n}_e}{\bar{n}_j}f_p^{-1}(n_e^s + n_{oj}^s) - (1+n_j^c)\left[2\bar{P}_j' + \bar{v}_{\phi j} - \frac{2\bar{E}_r}{\bar{B}_\theta}\right], \tag{19b}$$

where $L_\Phi^{-1} \equiv \bar{E}_r/\Phi^0 = -(\partial\Phi^0/\partial r)/\Phi^0$, $\bar{P}_j' = (1/\bar{n}_j e_j \bar{B}_\theta)\partial\bar{p}_j/\partial r$, and the electron density asymmetries are related to the ion density asymmetries by charge neutrality,

$$n_e^{c,s} = \frac{Z_j\bar{n}_j n_j^{c,s} + Z_k\bar{n}_k n_k^{c,s}}{Z_j\bar{n}_j + Z_k\bar{n}_k} \equiv \gamma_j n_j^{c,s} + \gamma_k n_k^{c,s}. \tag{20}$$

Making such low-order Fourier series expansions in the poloidal momentum balance Eq. (1) and taking the flux surface average results in a pair of coupled equations for the poloidal velocities,

$$\begin{aligned}
&\hat{v}_{\theta j}\left[-q\hat{v}_{\phi j}\varepsilon\tilde{n}_j^s + q^2 f_j f_p\left(1 + \frac{2}{3}\tilde{n}_j^c\right) + f_p\nu_{jk}^* + f_p\nu_{\text{atom}j}^*\right] \\
&\quad - \hat{v}_{\theta k}\nu_{jk}^*\sqrt{\frac{m_j}{m_k}}f_p \\
&\quad = -\hat{D}_{rj} - q\varepsilon\frac{1}{4}\tilde{n}_j^s + \frac{1}{4}q\varepsilon Z_j\frac{T_e}{T_j}[\tilde{n}_j^s\tilde{n}_e^c - (1+\tilde{n}_j^c)\tilde{n}_e^s] \\
&\qquad + q^2 f_j f_p\hat{E}_{rj} - \frac{1}{2}q\varepsilon\hat{v}_{\phi j}^2\tilde{n}_j^s + \hat{\nu}_{\text{ion}j}\left[\frac{2}{3}q^2 f_j(\tilde{n}_e^s + \tilde{n}_{oj}^s)\right. \\
&\qquad \left. - q\varepsilon f_p^{-1}(\tilde{n}_e^c + \tilde{n}_{oj}^c)\right] - \hat{L}_{\phi j}^{-1}[q^2 f_j f_p\tilde{n}_e^c + q\varepsilon\hat{v}_{\phi j}\tilde{n}_e^s],
\end{aligned} \tag{21}$$

where $\varepsilon = r/R$, $\hat{v}_{\theta j} = \bar{v}_{\theta j}/f_p v_{thj}$, $\hat{v}_{\phi j} = \bar{v}_{\phi j}/v_{thj}$, $\hat{P}'_j = \bar{P}'_j/v_{thj}$, $\tilde{n}_j^{s,c} = n_j^{s,c}/\varepsilon$, $\hat{E}_{rj} = \bar{E}_r/v_{thj}B_\theta$ $\hat{\nu}_{\mathrm{ion}j} = (r\bar{\nu}_{\mathrm{ion}j}/v_{thj})\bar{n}_e/\bar{n}_j$, and $\hat{L}_{\phi j}^{-1} = L_\phi^{-1}T_e/eB_\theta v_{thj}$. A similar equation with the "j" and "k" subscripts interchanged is obtained for the impurity species.

The atomic physics momentum transfer frequency $\nu_{\mathrm{atom}} = \nu_{elcx} + \nu_{\mathrm{ion}}$ consists of a momentum loss rate term due to charge-exchange and elastic scattering that enters the momentum balance directly plus an ionization term that enters via the inertia term. The friction terms are identified by $\nu_{jk}^* = \nu_{jk}qR/v_{thj}$, and the viscosity terms resulting from the use of the Shaing–Sigmar[6] expression $\eta_{0j} = n_j m_j v_{thj} qR f_j(\nu_{jj}^*)$ are identified by $f_j = \varepsilon^{-3/2}\nu_{jj}^*/(1+\varepsilon^{-3/2}\nu_{jj}^*)(1+\nu_{jj}^*)$, both in Eq. (21) and in Eqs. (23) and (24) below.

The electron momentum balance can be solved for $\Phi^0\tilde{\Phi}^{c/s} \equiv \Phi^0\Phi^{c/s}/\varepsilon = n_e^{c/s}/\varepsilon(e/T_e)$, which represents the poloidal asymmetry in the electrostatic potential. The FSA of the electrostatic potential, Φ^0, is conventionally determined by integrating the radial electric field radially inward from $\Phi^0 = 0$ at the first grounded (in contact with the vessel) field line, but the equations are independent of the normalization of Φ^0, which enters only as the product $\Phi^0\tilde{\Phi}^{c/s} = n_e^{c/s}/\varepsilon(e/T_e)$ or as the logarithmic derivative $L_\Phi^{-1} = -(\partial\Phi^0/\partial r)/\Phi^0$.

The term

$$\hat{D}_{rj} \equiv \frac{e_j B_\phi}{m_j v_{\mathrm{th}j}}\frac{qR}{v_{\mathrm{th}j}}v_{rj} + \frac{f_j q^2 B_\phi}{v_{\mathrm{th}j}}\frac{K^j T_j L_{Tj}^{-1}}{e_j B^2} \equiv \hat{v}_{rj} + \frac{f_j q^2 B_\phi}{v_{\mathrm{th}j}}\frac{K^j T_j L_{Tj}^{-1}}{e_j B^2} \tag{22}$$

represents the poloidal rotation driving forces from the V×B force and from the heat flux contribution to the parallel viscous force.

The $\tilde{n}^{s,c} = n^{s,c}/\varepsilon$ represent the poloidally asymmetric density components, which can be obtained by solving the equations resulting from taking the sin θ and cos θ FSA moments of the poloidal momentum balance Eq. (1),

$$\begin{aligned}
&\tilde{n}_j^s\left[\frac{q^2}{\varepsilon}f_j f_p\left(\frac{1}{3}\hat{v}_{\theta j} + \frac{1}{2}\hat{P}_j - \frac{1}{2}\hat{E}_{rj} - \frac{1}{2}\hat{L}_{\phi j}^{-1}\right) + \frac{1}{2}\varepsilon\hat{v}_{rj} - \frac{1}{2}\varepsilon f_p\left(\nu_{jk}^*\sqrt{\frac{m_j}{m_k}}\hat{v}_{\theta k} - \nu_{\mathrm{atom}j}^*\hat{v}_{\theta j}\right) + \frac{1}{2}qf_p\hat{v}_{\theta j}\hat{\nu}_{\mathrm{ion}j}\gamma_j\right] \\
&\quad + \tilde{n}_j^c\left[\frac{1}{2}qf_p^2\hat{v}_{\theta j}^2 - \frac{1}{4}q - \frac{1}{4}qZ_j\frac{T_e}{T_j}\gamma_j - \frac{1}{3}\frac{q^2 f_j}{\varepsilon}\hat{\nu}_{\mathrm{ion}j}\gamma_j\right] + \tilde{n}_k^s\left[\frac{1}{2}\varepsilon f_p\nu_{jk}^*\hat{v}_{\theta j} + \frac{1}{2}qf_p\hat{v}_{\theta j}\gamma_k - \frac{1}{2}\frac{q^2 f_j f_p}{\varepsilon}\hat{L}_{\phi j}^{-1}\gamma_k\right] \\
&\quad + \tilde{n}_k^c\left[-\frac{1}{3}\frac{q^2 f_j}{\varepsilon}\hat{\nu}_{\mathrm{ion}j}\gamma_k - \frac{1}{4}qZ_j\frac{T_e}{T_j}\gamma_k\right] = -\left[\frac{1}{2}qf_p^2\hat{v}_{\theta j}^2 + \frac{1}{2}q\hat{v}_{\phi j}^2 + \hat{\nu}_{\mathrm{ion}j}\left(\frac{1}{2}qf_p^2\hat{v}_{\theta j}\tilde{n}_{oj}^s + \frac{1}{3}\frac{q^2 f_j}{\varepsilon}\tilde{n}_{oj}^c\right)\right]
\end{aligned} \tag{23}$$

and

$$\begin{aligned}
&\tilde{n}_j^s\left[-\frac{1}{2}qf_p^2\hat{v}_{\theta j}^2 + \frac{1}{4}q + \frac{1}{4}qZ_j\frac{T_e}{T_j}\gamma_j + \frac{1}{3}\frac{q^2 f_j}{\varepsilon}\hat{\nu}_{\mathrm{ion}j}\gamma_j\right] + \tilde{n}_j^c\left[\frac{q^2}{\varepsilon}f_j f_p\left(\frac{1}{3}\hat{v}_{\theta j} + \frac{1}{2}\hat{P}_j - \frac{1}{2}\hat{E}_{rj} - \frac{1}{2}\hat{L}_{\phi j}^{-1}\right)\right. \\
&\quad \left. + \frac{1}{2}\varepsilon\hat{v}_{rj} - \frac{1}{2}\varepsilon f_p\left(\nu_{jk}^*\sqrt{\frac{m_j}{m_k}}\hat{v}_{\theta k} - \nu_{\mathrm{atom}j}^*\hat{v}_{\theta j}\right) + \frac{1}{2}qf_p\hat{v}_{\theta j}\hat{\nu}_{\mathrm{ion}j}\gamma_j\right] + \tilde{n}_k^s\left[\frac{1}{3}\frac{q^2 f_j}{\varepsilon}\hat{\nu}_{\mathrm{ion}j}\gamma_k + \frac{1}{4}qZ_j\frac{T_e}{T_j}\gamma_k\right] \\
&\quad + \tilde{n}_k^c\left[\frac{1}{2}\varepsilon f_p\nu_{jk}^*\hat{v}_{\theta j} + \frac{1}{2}qf_p\hat{v}_{\theta j}\gamma_k - \frac{1}{2}\frac{q^2 f_j f_p}{\varepsilon}\hat{L}_{\phi j}^{-1}\gamma_k\right] \\
&= -\left[\frac{1}{2}q^2 f_j f_p(\hat{v}_{\theta j} + \hat{P}'_j - \hat{E}_{rj}) + \hat{\nu}_{\mathrm{ion}j}\left(\frac{1}{2}qf_p^2\hat{v}_{\theta j}\tilde{n}_{oj}^c + \frac{1}{3}\frac{q^2 f_j}{\varepsilon}\tilde{n}_{oj}^s\right) + \frac{1}{4}q\varepsilon^2((\hat{v}_{\phi j}\tilde{v}_{\phi j}^s)(\hat{v}_{\phi j}\tilde{v}_{\phi j}^c))\right]
\end{aligned} \tag{24}$$

plus a similar set of equations with the "j" and "k" subscripts interchanged for the impurity species.

It should be noted that Eqs. (21), (24), and (25) constitute a set of six (three times the number of ion species) nonlinear equations, within which terms have been normalized and grouped to facilitate numerical solution by iteration. These equations extend the previous Stacey–Sigmar model for poloidal rotation (e.g., as described in Ref. 3) by using the extended parallel viscous force of Eq. (14) in place of Eq. (12), which introduces the temperature gradient driving term [the second term on the right in Eq. (22)] that was not present in the earlier work.

In order to more directly compare this poloidal rotation calculation model with an extended version of the Hirshman–Sigmar model that will be developed in the next section, we develop a reduced version by neglecting the poloidal asymmetries in density, rotation velocity, etc. (which are not included in the HS viscosity model) but retaining the poloidal asymmetry in magnetic field, $B = B_0/(1+\varepsilon\cos\theta)$ and major radius $R = R_0(1+\varepsilon\cos\theta)$ that has been used above. This reduces the inertial term in the poloidal momentum balance to the $\nu_{\mathrm{ion}j}$ term and eliminates the pressure gradient and poloidal electric fields terms. In this further approximation, the pair of Eqs. (21) reduces to

$$\left[\frac{q\upsilon_{\mathrm{th}j}f_j}{R}+\nu_{jk}+\nu_{\mathrm{atom}j}\right]\upsilon_{\theta j}-\nu_{jk}\upsilon_{\theta k}$$
$$=-\frac{e_j\upsilon_{rj}B_\phi}{m_j}+\frac{\upsilon_{\mathrm{th}j}f_jq}{R}\left(\frac{B_\phi K^j T_j L_{Tj}^{-1}}{e_jB^2}+\frac{\upsilon_{\mathrm{th}j}E_r}{B_\theta}\right) \quad (25)$$

and a similar equation with the "*j*" and "*k*" subscripts interchanged, which clearly displays the role of radial particle flows (V×B force), radial temperature derivatives (heat flux contribution to viscous force), and the radial electric field (flow contribution to viscous force) in driving poloidal velocity and the role of viscosity, friction, and ionization and charge-exchange of nonrotating neutrals in damping the rotation.

Diverse phenomena not usually found in poloidal rotation models are represented in the above equations. Atomic physics effects are explicitly indicated by the $\nu_{\mathrm{ion}}^*, \nu_{elcx}^*, \nu_{\mathrm{atom}}^*=\nu_{\mathrm{ion}}^*+\nu_{elcx}^*$ terms. The ionization of recycling neutrals also causes the deuterium υ_r to increase rapidly with radius just inside the separatrix, because $\Gamma=n\upsilon_r$ must increase with radius to satisfy the continuity equation, while n is decreasing rapidly in the same edge pedestal region. A poloidal electrostatic field is created in response to the density asymmetries in satisfaction of the Maxwell–Boltzmann constraint (electron poloidal momentum balance). The radial electric field was introduced via Eq. (18) from rotation velocities in the rate-of-strain tensor. We find that these novel effects are important in the calculations to be discussed later.

V. EXTENDED HIRSHMAN–SIGMAR POLOIDAL ROTATION THEORY

Following the same procedures as used in the preceding section, we extend the Hirshman–Sigmar theory to include terms in the poloidal momentum balance of Eq. (1) other than the viscous and friction terms. If we do not include poloidal asymmetry, which was not included in the original Hirshman–Sigmar viscous force, then the poloidal pressure gradient and poloidal electric field terms vanish, and we obtain a form similar to Eq. (25) but with the HS viscosity representation

$$\left[\nu_{jj}\frac{B}{B_\theta}\mu_{00}^j+\nu_{jk}+\nu_{\mathrm{atom}j}\right]\upsilon_{\theta j}-\nu_{jk}\upsilon_{\theta k}$$
$$=-\frac{e_j\upsilon_{rj}B_\phi}{m_j}+\nu_{jj}\frac{B}{B_\theta}\mu_{00}^j\left(\frac{B_\phi K^j T_j L_{Tj}^{-1}}{e_jB^2}\right) \quad (26)$$

plus a similar equation with the "*j*" and "*k*" subscripts interchanged. This extended form of the HS theory includes atomic physics, inertial, and V×B effects not present in the original theory discussed in an earlier section.

VI. NUMERICAL COMPARISON OF POLOIDAL VELOCITY THEORIES

Numerical calculations were carried out using several of the sets of equations described in this paper in order to compare differences in predictions of the different theories. In addition, a sensitivity study was performed to assess the importance of various physical phenomena to the calculated results. In order that the numerical comparison be based on a realistic model, experimental data from the outer 15% of a DIII-D discharge in which background plasma[10] and poloidal rotation data[11] have been analyzed were used to model the plasma for the rotation calculations.

DIII-D discharge 119436 was run in a lower single null divertor (SND) configuration with plasma current $I_p=1.0$ MA, toroidal field $B_t=1.6$ T, and average triangularity $\delta=0.35$. During the time of interest (3.0–3.5 s), the injected beam power P_{beam} was 4.3 MW, the line-averaged density $\langle n_e\rangle$ was about 0.34×10^{20} m^{-3}, the global stored energy W_{MHD} was about 0.55 MJ, and the average ELM (edge localized mode) period was 15.3 ms. Even though the global parameters, such as $\langle n_e\rangle$ and W_{MHD}, were approximately constant during the time of interest, the conditions in the pedestal were constantly changing due to the effect of ELMs. The period 80–99% between ELMs was chosen for analysis for this shot. Data measured in this time interval just before the ELM (i.e., the last 20% of the time between successive ELMs) for several successive inter-ELM periods were averaged to minimize random measurement errors.[10,11] Experimental data for electron and carbon densities and for ion and electron temperatures were available, and experimental E_r's were constructed from measured carbon pressure gradients and poloidal and toroidal rotation as per Eq. (18). The experimental E_r was integrated inward from the separatrix and used to construct an experimental L_φ.

An integrated modeling code[12] was used to supplement the experimental data. This code (i) calculated particle and power balances on the core plasma to determine the net particle and heat outfluxes from the core into the scrape-off layer (SOL), calculated using measured confinement times, which were input to (ii) an extended two-point divertor plasma model (with radiation and atomic physics) that calculated densities and temperatures in the SOL and divertor and the ion flux incident on the divertor plate, which (iii) was recycled as neutral atoms and molecules that were transported through the 2D divertor region across the separatrix to fuel the core plasma.

The deuterium and carbon poloidal rotation profiles calculated with the extended Hirshman–Sigmar model of Eqs. (26), with the extended Stacey–Sigmar model of Eqs. (21)–(24), with the reduced Stacey–Sigmar model of Eqs. (25), and with the Kim–Diamond–Groebner model of Eqs. (7) and (8) are shown in Figs. 1 and 2. Also shown is the measured poloidal rotation for carbon. The Hirshman–Sigmar model is in best agreement with experiment overall. However, since the uncertainty in the measurement is comparable to the magnitude of the measured velocity, this comparison can only indicate that the calculated values are of the same magnitude as measured values. The overprediction of the rotation right at the separatrix by all the models is probably real and due to failure to take into account some edge phenomena such as particle scrape-off.[13] However, the purpose of these calculations is to compare the various theoretical models, not to compare with experiment, and we will defer to a later time following up on this observation.

The extended SS models of Eqs. (21)–(24) and the reduced SS model of Eq. (25), and to a lesser degree the

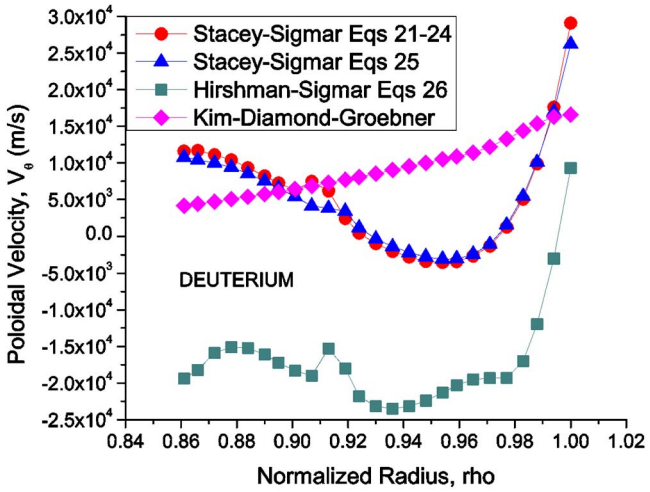

FIG. 1. (Color online) Comparison of deuterium poloidal rotation velocity predicted in the edge of a DIII-D discharge by various neoclassical theories.

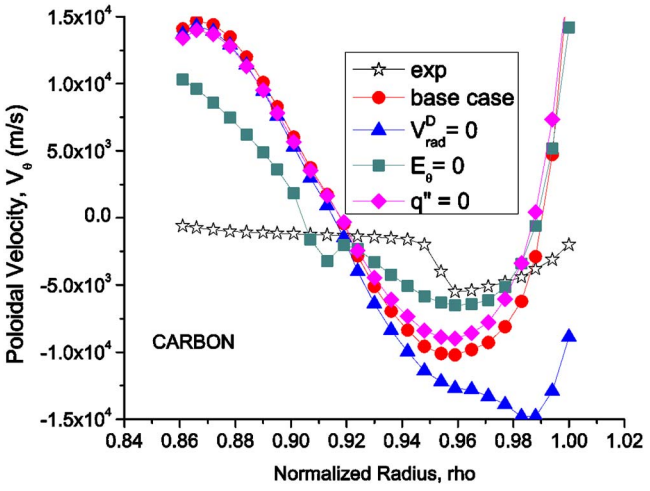

FIG. 3. (Color online) Sensitivity of predicted poloidal rotation velocity [Eqs. (21)–(24)] to inclusion of the V×B force, the poloidal electric field, and the heat flux component of the viscous force.

Hirshman–Sigmar model of Eq. (26), predict a strong negative peaking of the poloidal rotation in the edge pedestal "transport" barrier. Such peaking is commonly found in the poloidal rotation measurements in DIII-D.[14] Note that the positive sense of the poloidal rotation is taken in the right-hand sense with respect to the plasma current, which is down at the outboard midplane in this discharge (opposite sense from the experimental convention on DIII-D).

There is very little difference between the predictions of the extended Stacey–Sigmar model of Eqs. (21)–(24) and the reduced SS model of Eqs. (25) obtained by "turning off" all poloidal asymmetries, which perforce neglects poloidal pressure gradients and electric field, as well as poloidal effects on the viscous and inertial forces.

Differences in the predictions of the reduced SS model of Eqs. (25) and the extended HS model of Eq. (26) are due to differences in viscous forces used in the two models, as given by Eqs. (14) and (5), respectively. Note that the poloidal asymmetry effects are not present in the reduced SS model. The carbon rotation velocities predicted by the two models are similar (and similar to the measured velocity), but the deuterium velocities predicted by the two models differ considerably (even have different signs).

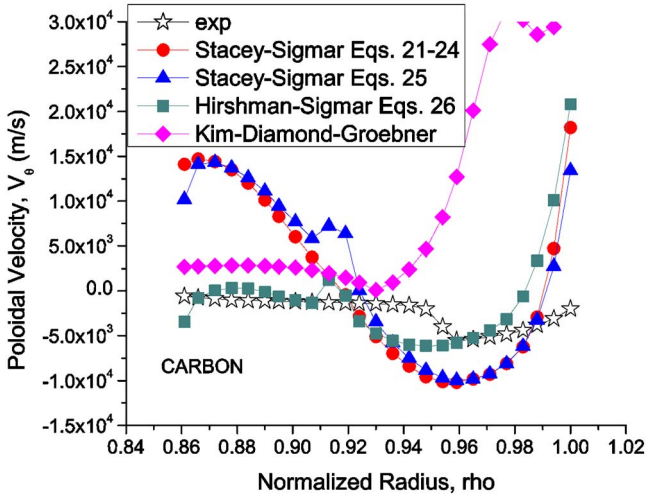

FIG. 2. (Color online) Comparison of carbon poloidal rotation velocity predicted in the edge of a DIII-D discharge by various neoclassical theories and the measured poloidal velocity.

Predictions of the Kim–Diamond–Groebner model of Eqs. (7) and (8) are at considerable variance with the other predictions (and with the measured velocity), indicating that it is necessary to retain more terms than just the friction and main ion viscous terms in the momentum balance Eqs. (1).

Separate predictions were calculated from the extended SS Eqs. (21)–(24) with $V_{\mathrm{rad}}=0$, with $E_\theta=0$, and with the heat flux contribution to the viscous force removed ($q"=0$). The predicted velocities are compared with "base" prediction of these equations when both V_{rad} and E_θ were calculated as described previously and the heat flux was included in the viscous force. V_{rad} for deuterium increases strongly near the separatrix because of the ionization of recycling and fueling neutrals, and elimination of this driving term from the right side of Eq. (21) significantly reduces the rotation velocity of both species near the separatrix, as shown in Fig. 3 for carbon. Setting $E_\theta=0$ but retaining other poloidal asymmetry effects has a significant effect on the magnitude of the predicted negative velocity peaking in the transport barrier, as also shown in Fig. 3. Note that when $E_\theta=0$ and all other poloidal asymmetries were also set to zero, the net effect on the solution was negligible, as shown by comparison of the two SS calculations in Figs. 1 and 2, indicating that there is a compensating effect among the different poloidal asymmetry effects. When the heat flux term in the viscous force [the second term in the square brackets in Eq. (14)] was set to zero, there was only a small effect on the predicted rotation velocities, as shown for carbon in Fig. 3.

VII. SUMMARY

It was shown that several of the extant neoclassical theories for poloidal rotation can be derived from the same fluid poloidal momentum balance equation by retaining different

terms and using different expressions for the parallel viscous force. This suggested several natural extensions of these theories.

Numerical calculations were performed to compare the predictions of the theories and to examine the effect of various phenomena on the prediction of poloidal rotation velocities. Inclusion of terms other than just the viscous and friction forces in the derivation of theoretical formulas for the poloidal rotation was found to be important. In particular, the $V \times B$ force due to the strong radial particle flux buildup in the edge due to ionization of recycling neutrals was found to significantly affect the poloidal rotation, and the inclusion of the poloidal electric field and the heat flux contribution to the viscous force were found to have smaller effects.

[1]R. D. Hazeltine, Phys. Fluids **17**, 961 (1974).
[2]S. P. Hirshman and D. J. Sigmar, Nucl. Fusion **21**, 1079 (1981).
[3]W. M. Stacey, Phys. Plasmas **9**, 3874 (2002); Contrib. Plasma Phys. **46**, 597 (2006).
[4]B. Kim, P. H. Diamond, and R. J. Groebner, Phys. Fluids B **3**, 2050 (1991).
[5]W. A. Houlberg, K. C. Shaing, S. P. Hirshman, and M. C. Zarnstorff, Phys. Plasmas **4**, 3230 (1997).
[6]W. M. Stacey, A. W. Bailey, D. J. Sigmar, and K. C. Shaing, Nucl. Fusion **25**, 463 (1985).
[7]W. M. Stacey and D. J. Sigmar, Phys. Fluids **28**, 2800 (1985).
[8]W. M. Stacey, Phys. Fluids B **4**, 3302 (1992).
[9]S. I. Braginskii, Rev. Plasma Phys. **1**, 205 (1965).
[10]W. M. Stacey and R. J. Groebner, Phys. Plasmas **14**, 122504 (2007).
[11]W. M. Stacey and R. J. Groebner, "Interpretation of edge pedestal rotation measurements in DIII-D," Phys. Plasmas (to be published).
[12]W. M. Stacey, Phys. Plasmas **5**, 1015 (1998); **8**, 3673 (2001); Nucl. Fusion **25**, 463 (2000).
[13]R. Hiwatari, T. Takizuke, K. C. Shaing *et al.*, Plasma Phys. Controlled Fusion **44**, A445 (2002).
[14]R. J. Groebner, General Atomics (personal communication).